Indonesian Journal of Science & Technology 7(2) (2022) 187-202

Indonesian Journal of Science & Technology

Journal homepage: http://ejournal.upi.edu/index.php/ijost/

Amorphous Iron Phosphate: Inorganic Sol-Gel Synthesis-Sodium and Potassium Insertion

Fatima-Ezzahra Maarouf [1], Sanaa Saoiabi [1], Khalil Azzaoui [2], Hind Khalil [1], Mariam Khalil [1], Ahmed El Yahyaoui [1], Ahmed Saoiabi [1], Belkheir Hammouti [2,3*], Moulay Hfid Youssoufi [2], Sergey Shityakov [4], Othman Hamed [5], Shehdeh Jodeh [5], Rachid Sabbahi [6]*

[1] Laboratory of Applied Chemistry of Materials, Department of Chemistry, Faculty of Sciences, Mohammed V University in Rabat, Morocco.
[2] Laboratory of Applied Chemistry and Environment LCAE, Faculty of Sciences, First Mohammed University, PO Box 717, 60 000 Oujda, Morocco.
[3] Ecole des Hautes Etudes d'Ingénierie EHEI, 60000 Oujda Morocco
[4] Department of Bioinformatics, Würzburg. University, 97074 Würzburg, Germany
[5] Department of Chemistry, College of Science, An-Najah National University, Nablus, Palestinian Territories.
[6] University of Ibn Zohr, Higher School of Technology, Laayoune, Morocco, and Faculty of Sciences, Laboratory of Plant Biotechnology, Agadir, Morocco.
*sCorresponding author, email: sanaa.saoiabi@yahoo.com, hammoutib@gmail.com

ABSTRACT

Amorphous iron phosphate, $FePO_4.2H_2O$, was synthesized at ambient temperature using an inorganic sol-gel method coupled with a microwave route. The experimental conditions for the gelling of the Fe (III)-H_3PO_4 system are defined. Potentiometric Time Titration (PTT) and Potentiometric Mass Titration (PMT) methods were used to investigate the acid-base surface chemistry of obtained phosphate. Variations of surface charge with the contact time, Q = f(t), are examined for time contact ranged from 0 to 72 hours. The concentrations suspensions used for this purpose were 0.75, 1.25, and 2.5 g/L. The point of zero charges (PZC) and isoelectric point (IEP) were defined using the derivative method examining the variations $\frac{dpH}{dt} = f(pH)$, at lower contact time. A value of 5.4 was obtained for both PZC and IEP. Q in the function of the t method is performed for synthesized $FePO_4$. $2H_2O$ in NaCl and KCl electrolytes. The optimal surface charge of 40 C corresponding to insertion of $4.2x10^{-4}$ M of Na^+ or K^+, is achieved in explored conditions. The results suggest that the synthesized iron phosphate is amorphous.

© 2022 Tim Pengembang Jurnal UPI

ARTICLE INFO

Article History:
Submitted/Received 10 Feb 2022
First revised 19 Mar 2022
Accepted 10 May 2022 First available online 16 May 2022
Publication date 01 Sep 2022

Keyword:
Amorphous,
Engineering,
IEP,
Inorganic sol-gel,
Iron phosphate,
PZC,
Sodium and potassium insertion,
Surface charge,
Surface property.

1. INTRODUCTION

Rechargeable batteries are of important concern and are considered the most promising energy storage system, especially for mobility (electric vehicle) and large-scale (gird level) energy storage applications, owing to the high energy density, and cycle life compared to other storage systems (Ramesh *et al.*, 2019). For these batteries, surface processes are important and limit their application space, so it has been proposed to substitute the lithium metal anode with an insertion electrode. Indeed, insertion-type materials possess better cyclic stability than alloy-type that is widely investigated for their potential use as an electrode (Zhang *et al.*, 2018; Gabaudan *et al.*, 2019). The insertion of these materials, including oxides or phosphates, was performed from electrolytes consisting of the alkali ions. It can be noted that amorphous compounds with short-range ordering are more convenient for the insertion of various ions, without a phase transition. Due to the high surface area and free volume of these products and stable electrochemical cycling was achieved over a wide potential range (Vinod *et al.*, 2015). Transition metal phosphates are an important class of inorganic products that are intensively investigated for their low-cost, environmental friendliness, and biocompatibility. These phosphates are considered thermally stable materials, have a higher storage voltage, and are intensively investigated for large-scale applications including, electrochemical energy storage, catalysis, and water purification (Pan *et al.*, 2013).

Among these materials, iron (III) phosphates are long been used in the steel and glass industries and they have recently gained more interest in developing alkali ion batteries (Kazuhiko *et al.*, 2006). The ion insertion into electrode materials is dependent on the alkali ion diffusion and therefore, on the ionic conduction process. To improve this process, a large number of ions must be inserted into an electrode structure. Owing to the strong P-O bonds in metal (III) phosphates, the phosphorus atoms are inactive regarding the electrolyte medium, allowing thus, an easy movement of alkali metal ions in these matrices (Ramesh *et al.*, 2019). Moreover, it is reported that Li^+ diffusion and charging-discharging processes are improved in low crystalline phosphate (Kang & Ceder, 2009). Recently, with limited lithium resources, an important concern is emerged about sodium-ion as one of the promising substitute elements due to its natural abundance. However, the process of sodiation/ desodiation requires a large host space for Na^+ ions that are exhibiting a lower diffusion rate compared to Li^+. As a result, considerable efforts are been made to develop electrodes with lattice space suitable to insert sodium or potassium ions. To seek this purpose, phosphates with open-layered structures are required. Amorphous $FePO_4$ considered a conceptual defect-free phase, is widely reported as electrode material in lithium batteries, and is widely investigated as a host material for various charge carrier ions.

The results obtained show that the iron phosphate cathode exhibits a good reversible Na-ion storage capacity and allowed a fast pathway for sodium-ion transportation (Moradi *et al.*, 2015). As a result, Na-rich amorphous materials are suitable to develop a non-crystalline iron phosphate cathode material (Vinod *et al.*, 2015). These phosphates are among the most promising electrodes for sodium-ion batteries and are convenient for large-scale energy storage. The capacity retention of 66 to100 mA.h/g is achieved for amorphous $FePO_4$ materials. Also, the potassium-ion batteries are regarded as the upcoming generation battery due to the advantages of ubiquitous availability, fast ion transport kinetics in the electrolyte, and energy density of −2.93 V, comparable to −3.04 V of the lithium electrode (Vinod *et al.*, 2015; Wenchao *et al.*, 2019).

DOI: https://doi.org/10.17509/ijost.v7i2
p- ISSN 2528-1410 e- ISSN 2527-8045

Consequently, considerable efforts have been focused on the exchange and incorporation of alkaline ions into the channels or between the layers of hydrated phosphates. It is reported that the alkalinization (lithiation, sedation) route of these phosphates is carried out through a simplex H^+ /Li^+(Na^+) ion-exchange process. These wet chemistry methods are often known as "soft chemistry", and are performed in a non-aqueous medium, using an organic acid as a source of protons (Lozano-Calero *et al.*, 1993; Wang *et al.*, 2015. Errich *et al.*, 2021).

In aqueous-based systems, the electrochemical performance of alkaline ion batteries is controlled, in particular, by the surface chemistry of electrode materials. To improve the electrochemical properties of these electrodes, it is necessary to define surface parameters governing the alkaline route. The main phenomena involved in the surface chemistry of M (Li^+, Na^+, and K^+) $FePO_4$ are the acid-base reactions combined with the alkaline ion exchange process or the surface adsorption of charged species (Lee *et al.*, 2010). Besides, $FePO_4$ has pH-dependent surface charge properties, which allows it to be used as an efficient sorbent of various elements such as heavy metals (Li *et al.*, 2018).

Iron phosphate subsequently gains more and more interest as an effective sorbent for the control of water pollution, as well as for biological systems (NaeemáKhan *et al.*, 1993; Lenoble *et al.*, 2005; Thinnappan *et al.*, 2008; Xiao-Xing *et al.*, 2012). Although this extensive electrochemical use of Fe (III) phosphate, both surface chemistry, and sorption mechanisms remain relatively difficult to establish (Ahmed *et al.*, 2017). This phosphate considered a complex oxide contains surface OH groups of Fe_2O_3 which a Point of Zero Charge (PZC) ranging from 6.3 to 8.5 for Goethite, and from 7.5 to 9.5 for Hematite, and P_2O_5 oxides which PZC value is about -3.4 (Weinheim & Kosmulski, 2004; Valérie & Rudy, 2008). Thus, the net surface charge of $FePO_4$ is the algebraic sum of the negative charge on the more basic sites (PO_4^-), and the positive charge on the more acid sites ($FeOH_2^+$) (Tejedor-Tejedor & Anderson, 1990; Abram & Alberto, 2006). Therefore, the point of zero charges of these phosphates is controlled by the quotient (R) of Fe to P atoms and diminishes with R decreasing (Ai & Ohdan, 1999). As found previously, PZC or the isoelectric point shift with contact time from 8.8 to 3.3, respectively for a duration equal to 0 and higher than 30 min.

The shift occurring at a higher duration is assumed to be due to the bridging surface complexes of type $>FeHPO_4H_2$ (Tejedor-Tejedor & Anderson, 1990; Ikram *et al.*, 1998; Nils Nilsson et al., 2012). In addition, metal phosphates exhibit higher adsorption properties, owing to their phosphorus framework, and porous structure that is more convenient for the mass transfer, due to reduced diffusion resistance. Despite the sorption results, the surface chemistry of these phosphates remains less explored, and shows low points of zero charge value ranging from 2.5 to 3.0, for $M(PO_4)_3$ materials such as $CePO_4$, $LaPO_4$, YPO_4, and $FePO_4$ (Mustafa *et al.*, 1999; Naeem *et al.*, 2001; Mustafa *et al.*, 2006). The low PZC value of 3.0 is reported for amorphous precipitated hydrous $FePO_4$ (De Tommaso & Iuliano, 2012). Synthesis and electrochemical characterization of iron phosphates have been carried out using precipitation methods (Palacios *et al.*., 2012), or hydrothermal techniques (Song *et al.*., 2002).

2. EXPERIMENT

2.1. Materials

All chemicals are of reagent quality, phosphoric acid (99%), iron (III) nitrate (99%), sodium hydroxide (NaOH) (99%), Nitric acid (HNO3) (99%), NaCl, and KCl were obtained from Sigma Aldrich Chemical Co. and were

DOI: https://doi.org/10.17509/ijost.v7i2
p- ISSN 2528-1410 e- ISSN 2527-8045

used as received without any further purificationx] High-purity distilled water was used for all experiments.

2.2. Methods

X-Ray Diffraction (XRD) data were collected at room temperature using an X-ray diffractometer (Siemens D 500) with copper anticathode radiation ($\lambda_{CuK\alpha}$=1.541838) at 2θ varying from 10 to 90°. Fourier Transform Infrared (FTIR) spectra were obtained on a Vertex 70 spectrometer equipped with a Digitec detector, via the conventional KBr pellet method. The simultaneous thermogravimetry and differential thermal analysis (TG/DTA) are performed using a LabsysTMEvo (1F) Setaram apparatus. Samples of an initial mass of 10 ± 0.4 mg are placed in an alumina crucible, and heated in an air atmosphere (60 mL/min) from ambient temperature up to 900 °C, using a heating rate of 10 °C/min.

2.3. Synthesis of Iron (III) Phosphate and Determination of PZC

Iron (III) phosphate was synthesized by a modified inorganic sol-gel method (El Yahyaoui *et al.*., 2002; Maarouf *et al.*., 2021). In this method, phosphoric acid (0.1 M) and iron (III) nitrate (0.1M) were used as the starting materials. The obtained mixture with Fe/P molar ratios of 1:1 was irradiated in a microwave oven (800 w) for about 15 sec. The resulting gel was oven-dried at 50 °C for about 48 hours. Obtained phosphate xerogels were repeatedly washed with distilled water and ethanol, and were identified as amorphous $FePO_4.xH_2O$ by the associated XRD patterns and FT-IR. The insoluble xerogel has been identified as completely amorphous by an X-ray powder diffraction (**Figure 1**). The batch equilibration technique is applied to determine the Point of Zero Charge (PZC). Surface charge variations Q = f(t), are examined at ionic strength (0.01 and 0.1 M. The iron phosphate of 0.75, 1.25, and 2.5 g/L was suspended in NaCl or KCl electrolyte.

3. RESULTS AND DISCUSSION

3.1. Characterization

The XRD patterns of synthesized powders are given in **Figure 1**. The insoluble precipitate has been identified as completely amorphous iron phosphate. FT-IR spectrum is shown in **Figure 2** and is normalized to the intensity of the (PO) (P–O stretching band) at 1085 cm^{-1}.

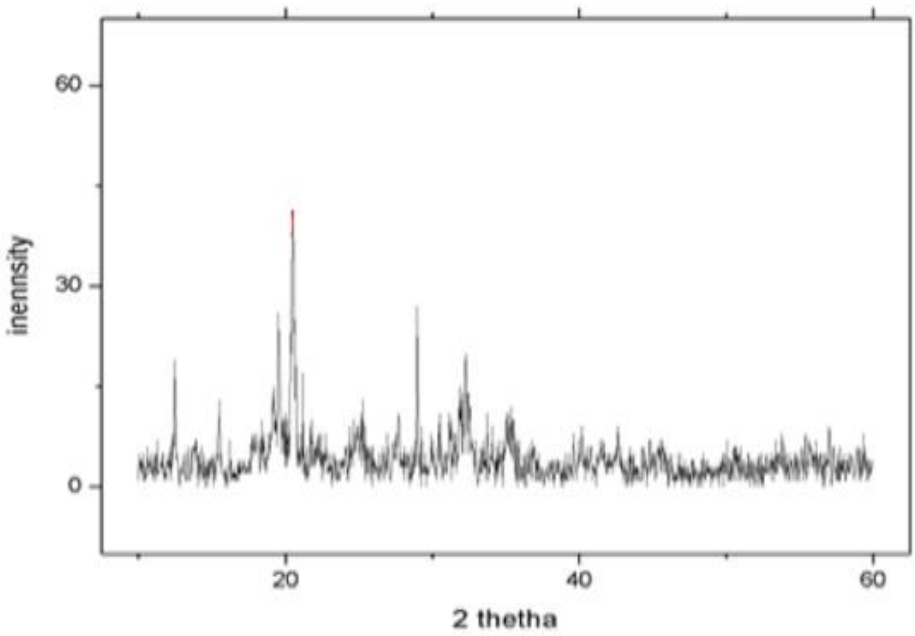

Figure 1. Diffractograms of xerogels obtained in Fe (III)-H_3PO_4 system.

DOI: https://doi.org/10.17509/ijost.v7i2
p- ISSN 2528-1410 e- ISSN 2527-8045

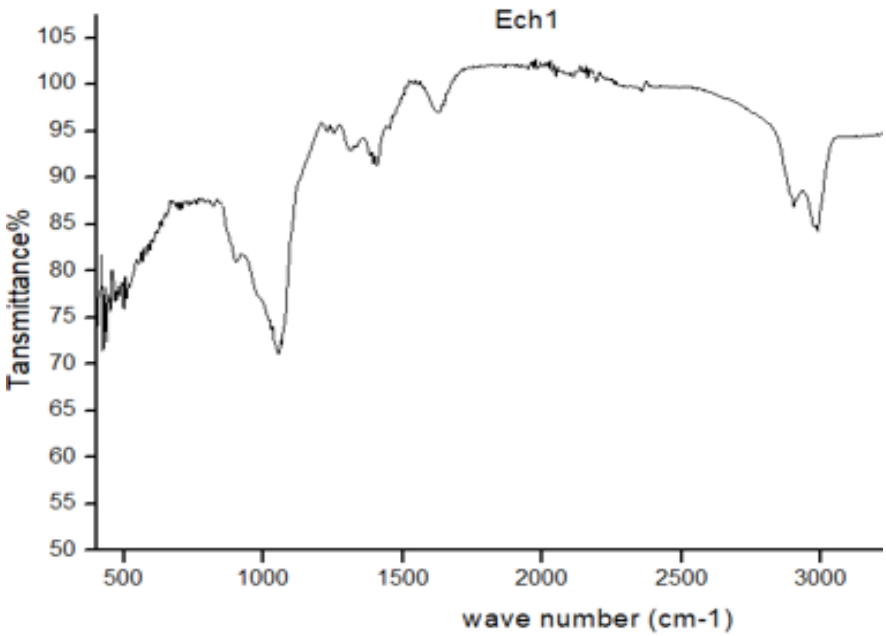

Figure 2. FTIR spectra of synthesized iron phosphate.

The vibration bands are assigned to the fundamental vibrating modes, namely PO_4^{3-} and H_2O. The bands in the 3600–2700 cm^{-1} region are attributed to the OH stretching vibrations of water, and hydroxyl groups of acid phosphate. The HOH bending band of sorbed water occurs at 1640 cm^{-1}.

The assignment of main Raman bands in the spectra of iron phosphates is listed in **Table 1** (Berzina-Cimdina and Borodajenko, 2012). The P–O stretching band appears around, 1000 cm^{-1}, and the shoulder at 900 cm^{-1} is associated with the O–P–O bending mode. Enlargement of the 1000 cm^{-1} band is observed with aging time, leading to higher wavenumbers shifts. This result is following XRD analysis, showing an increase in the P-O bond strengths associated with the formation of supplementary phosphate structural units**.**

As reported previously, an increase in iron phosphate acidity is also observed with aging time, which leads to the rising of the characteristic O–P–O bending peak at 900 cm^{-1} (Ellouzi *et al..*, 2016; Maarouf *et al..*, 2021). Two lower frequency bands occurring at 640 and 540 cm^{-1} are associated with bending modes of the structural OH groups and P–O bonds, respectively. The thermal analysis of phosphate material is carried out by DTA-TGA, results are shown in **Figure 3**.

Two endothermic peaks at 115 and 175°C are observed on the DTA curves. Rapid weight loss of 19.6 wt% on the TG curves is associated with quick dehydration of this phosphate that is consistent with the content of the crystalline water molecules in $FePO_4.2H_2O$. A second exothermic dehydration phenomenon with low weight loss is observed at temperatures of 370°C. As discussed previously, this dehydration process only concerns minor rearrangements of the framework, whereas the structure is not destroyed (Gongyan *et al..*, 2018).

An endothermic peak appearing at 590°C is corresponding to the phosphate condensation in which a hydroxyl polymerized chain is obtained. This polymerization is associated with a significant weight loss that is associated with amorphous pyrophosphate, as reported in the literature (Yong-ming *et al.*, 2014; Razzouki *et al.*, 2015). At higher temperatures, no appreciable weight loss is observed on the TG curves.

DOI: https://doi.org/10.17509/ijost.v7i2
p- ISSN 2528-1410 e- ISSN 2527-8045

Table 1. Assignment of main Raman bands in the spectra of iron phosphate.

Functional groups	Absorption bands, (cm^{-1})	Attribution
OH^-	3500 (Meejoo *et al.*, 2006) 630 and 3540 (Destainville *et al.*, 2003), 3570 and 3420 (Han *et al.*, 2006); 1650 (Raynaud *et al.*, 2002)	phosphate OH^- ions
Adsorbed water	2600 – 3600 (Meejoo *et al.*, 2006)	Under the influence of thermal treatment, the absorption band becomes narrower
HPO_4^{2-}	875 (Destainville *et al.*, 2003), (Raynaud *et al.*., 2002); 880 (Zhu *et al.*,2003)	Characterizes HAp with deficient calcium. (Raynaud *et al.*, 2002); Refers to non-stoichiometricHAp (Zhu *et al.*, 2003)
PO_4^{3-}	460 (Destainville *et al.*, 2003); (Raynaud *et al.*, 2002) (Destainville *et al.*, 2003);	ν_2 (Destainville *et al.*, 2003),
	560 - 600 (Destainville *et al.*, 2003), (Raynaud *et al.*, 2002), (Mobasherpour & Heshajin, 2007); 602 and 555 (Han *et al.*, 2006)	ν_4 (Destainville *et al.*, 2003); bending mode (Han *et al.*, 2006)
	960 (Destainville *et al.*, 2003), (Raynaud *et al.*., 2002)	ν_1 (Destainville *et al.*, 2003)
	1020-1120 (Destainville *et al.*, 2003), (Raynaud *et al.*, 2002); 1040 (Han *et al.*, 2006); 1000-1100 (Mobasherpour & Heshajin, 2007);	ν_3 (Destainville *et al.*, 2003);νbending mode (Han *et al.*, 2006);
NO_3^-	820 and 1380 (Destainville *et al.*, 2003); (Raynaud *et al.*, 2002)	Synthesis residue that disappears during the calcifying process (Destainville *et al.*, 2003)

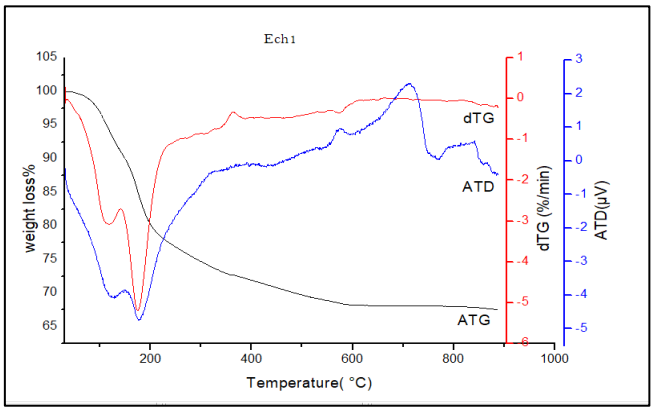

Figure 3. DTA–TGA of amorphous iron phosphate.

3.2. Scanning Electron Microscopy

The SEM technique is used to examine the surface physical morphology of iron phosphate. **Figure 4** shows the SEM images with 1000 x magnification and a scale bar of 10 µm. The micrograph shows that the particles are uniformly agglomerated and are exhibiting irregular morphology. The porous surface is resulting in a considerably agglomerated mesostructured, which is more convenient for the diffusion of metal ions into the phosphate matrix (Lee *et al.*, 2017; Salamani *et al.*, 2018). The composition and the purity of this synthesis phosphate are established using dispersive energy X-ray spectroscopy (EDX), the spectrum is presented in **Figure 5**. As shown, no impurities that can be attributable to contamination of chemical precursors are detected (Maarouf *et al.*, 2021).

DOI: https://doi.org/10.17509/ijost.v7i2
p- ISSN 2528-1410 e- ISSN 2527-8045

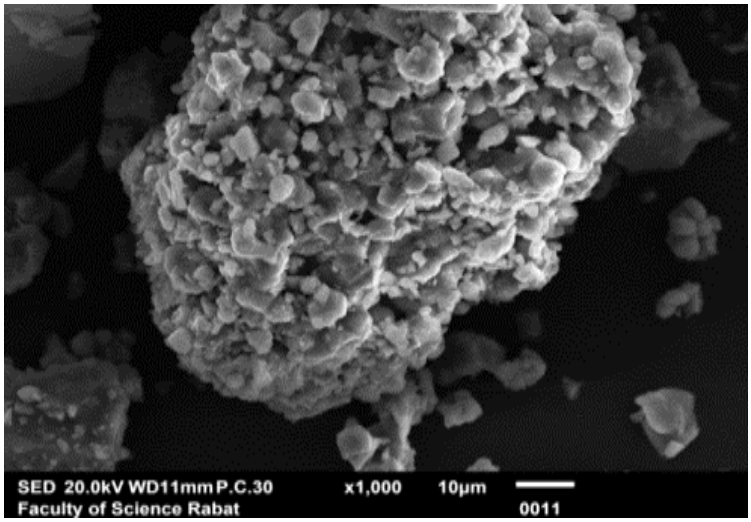

Figure 4. SEM image of synthesized $FePO_4.2H_2O$.

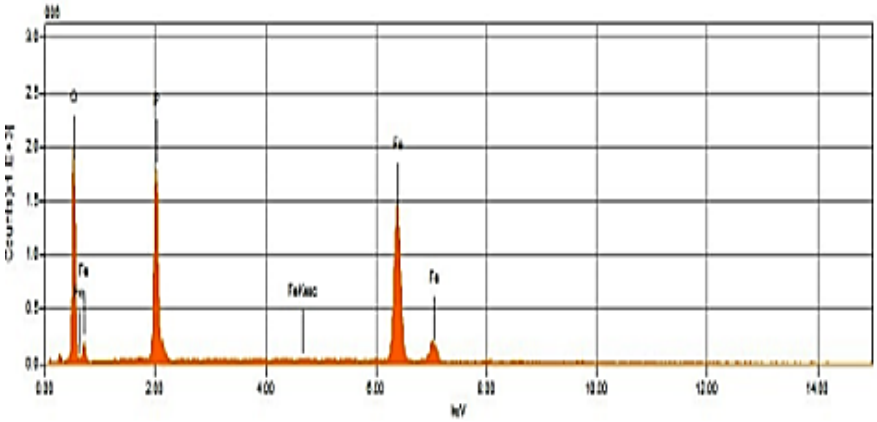

Figure 5. EDX spectra of synthesized iron phosphate.

3.3. Iron Phosphate Surface Chemistry and Sodium Inclusion

In general, the adsorption process is governed by the surface chemistry which involves acid-base interactions via the surface sites of the sorbent. As a result, the adsorption mechanism results in H^+ or OH^- ion-exchange reaction, and accordingly, it is more dependent on the pH of the suspension medium.

The surface hydroxyl groups involved in this exchange are resulting from the activation process carried out in the dissociation of chemisorbed water. As a result, the surface charge (*Q*) of a sorbent is associated with the concentration of protons or hydroxide ions and consequently, is dependent on the acidity of the suspension medium. *Q* is determined by a mass balance between the concentrations of H^+ or OH^- added to the solution, and that measured at a given contact time. For this purpose, desorbed protons on the phosphate surface are measured as a function of pH, hydration time (*T*), and sorbent mass (*m*).

According to the previous study (Jarlbring *et al.*, 2005; Jarlbring *et al.*, 2006; Ellouzi *et al.*, 2016; Maarouf *et al.*, 2021), the surface protonation/deprotonation reactions involved in metallic phosphate sorbents are well described as reactions of amphoteric acid-base surface groups ($\overline{>SOH}$) (see Equations [1] and [2]):

DOI: https://doi.org/10.17509/ijost.v7i2
p- ISSN 2528-1410 e- ISSN 2527-8045

$$\overline{>\mathrm{SOH}} + \mathrm{H}^+ \leftrightarrow \overline{>S(OH_2)^+}\ ,\ K^+ \qquad (1)$$

$$\overline{>SOH} \leftrightarrow \overline{>SO^-} + \mathrm{H}^+, K^- \qquad (2)$$

K^+ and K^- are the surface stability constants, and the on-lined species are referred to as the solid phase. For ferric phosphate, acid-base properties are attributed to protonation and deprotonation of phosphohydrolase ($\overline{>\mathrm{POH}} \equiv \overline{>S_1\mathrm{OH}}$) and the ferrihydrols ($\overline{>FeOH} \equiv \overline{>S_2\mathrm{OH}}$), which pK_a are 1.44 and 4.66, respectively (De Tommaso & Iuliano, 2012).

In this study, an electrochemical method is undertaken to examine the surface chemistry of synthesized Fe (III) phosphate. This method consists of potentiometric mass titration (PMT) and potentiometric time titration (PTT), which is performed in NaCl or KCl on 0.05 M HNO_3 dispersions. The sorbent amounts (m) are varying between 0 (blank) and 2.5 g/L, while suspension time (T) is ranging from 0.5 to 72 hours. The standard 0.05 M NaOH solution is used as a titrant.

3.4. Determination of Surface Charge

The mean surface charge is calculated, directly from the titration curves (pH=f(V)), according to the following Equation [3]:

$$Q = \frac{F(\mathrm{C_A} - \mathrm{C_B})\Delta V}{m}(\text{Coulomb/g}) \qquad (3)$$

where F is the Faraday constant, C_A and C_B are respectively the HNO_3 and NaOH concentrations that are of 0.05 M, ΔV is the difference in the volume of acid used to reach the same pH in dispersion and blank solution, and m (g/L) is the suspension concentration of the solid particuiles.

3.4.1. Phosphate Suspensions in NaCl Electrolyte

The Potentiometric Time Titration curves, Q in the function of pH of $FePO_4.H_2O$ suspensions are performed for m = 0.75, 1.25 and 2.5 g/L at interval time 0.5 h $\leq T \leq$ 72h. Surface titration curves showing the effect of contact time and ionic strength (μ) on the variation Q = f(pH) are reported in **Figures 6** and **7**. As shown in **Figures 6** and **7**, for a given mass of sorbent, the surface charge increases to reach a maximum and then decreases if contact time continues to rise. The similar variations shape of Q in the function of pH achieved at various contact times shows a plateau in pH of 3-11 confirming that these variations are not inferred to protonation or deprotonation process of $FePO_4.2H_2O$ surface. Asymptotic behavior is observed in all cases at pH around 13.4 $\pm$ 0.3.

As a result, the phosphate surface acquires, often, a positive charge as a consequence of the sorption of Na^+ ions. In all the cases, the zero-charge corresponding to PZC is found to be varying in the range between 3 and 10. Usually, this large range of PZC values is associated with amorphous materials (Muhammad *et al.*, 2012). As found, a maximal Q value of around 40 coulombs is obtained at a pH of about 12.

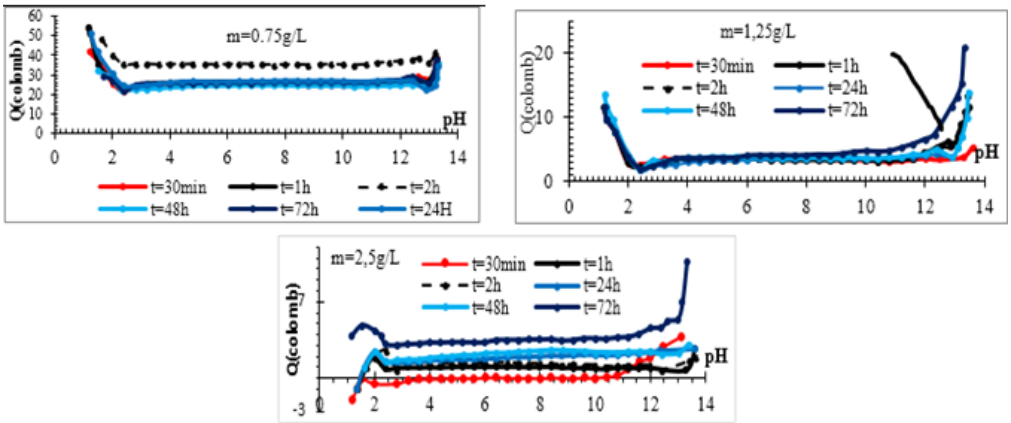

Figure 6. Variation Q = f (pH) for $FePO_4,2H_2O$ in KCl 0.001M, at $0.5h \leq T \leq 72h$ and $0.75gL^{-1} \leq m \leq 2.5gL^{-1}$.

DOI: https://doi.org/10.17509/ijost.v7i2
p- ISSN 2528-1410 e- ISSN 2527-8045

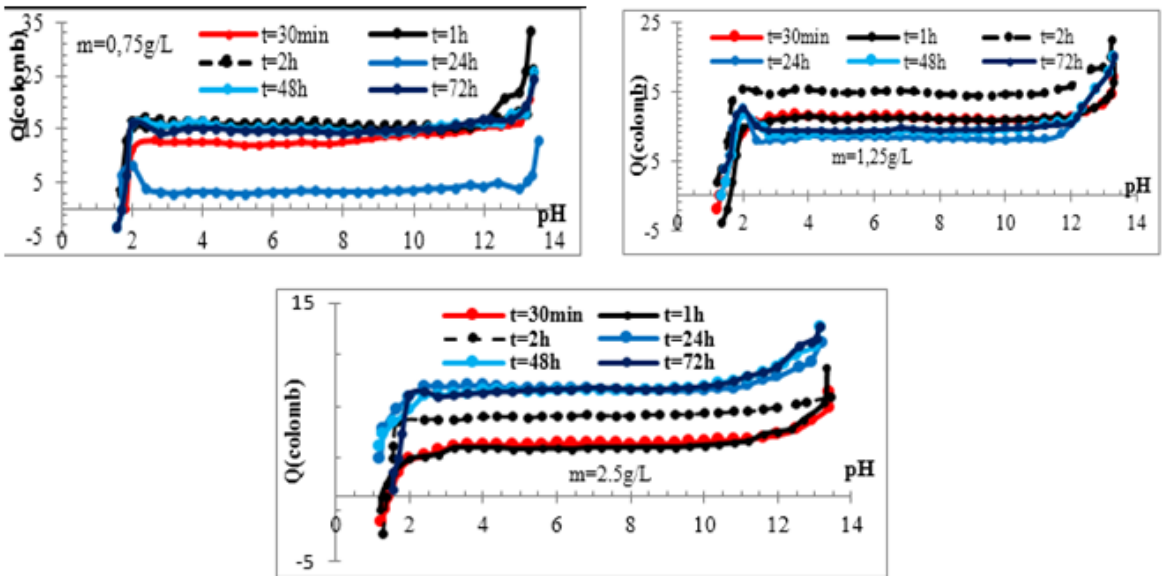

Figure 7. Variation Q = f (pH) for $FePO_4.2H_2O$ in NaCl 0.01 M at $0.5h \leq T \leq 72h$ and 0.75 g/L < *m* < 2.5 g/L.

This surface charge due to the insertion of $4.2.10^{-4}$ M of Na^+ is achieved for *m* = 0.75 g/L and NaCl concentrations of 0.01 and 0.1 M. The sodium ion insertion mechanism, however, is not enhanced with the increase in sorbent amount. In addition, the non-effect of μ on the PZC confirms the no association of electrolyte ions with both negative and positive sites of the $FePO_4$ surface.

3.4.2 Point of Zero Charge

To avoid electrolyte ion sorption, Isoelectric Point (IEP) determination is achieved at lower durations from pH = f(T) variations obtained for *m* = 0.75 g/L of iron phosphate suspensions. The variation of $\frac{\mathrm{dpH}}{\mathrm{dt}} = \mathrm{f(pH)}$ is shown in **Figure 8**.

As shown in **Figure 8**, $\frac{\mathbf{dpH}}{\mathbf{dT}} = \mathbf{f(pH)}$ curves are intersecting with each other at a single point located on the x-axis. As a result, this point corresponds to both the isoelectric point and point of zero charges whose value is IEP = PZC = 5.4. For pH ranging from 7 to 10, values around zero are obtained for $\frac{\mathbf{dpH}}{\mathbf{dT}}$ suggesting that constant surface charge *Q* is obtained in these pH conditions.

3.4.3. Phosphate Suspensions in KCl Electrolyte

Values of surface charge are obtained from pH-titration at various ionic strengths μ of KCl electrolyte salt **(Figures 9, 10, and 11)**.

In all the cases, *Q* in the function of the pH curve shows an inflection point at pH around 2, remains almost constant up to a pH of about 12, and then increases sharply when the pH continues to rise.

As found for NaCl, the highest Q values are achieved at pH around 13.4 ± 0.3 for all samples. The permanent surface charge arises from hydroxyl functional groups, while the variable positive charge is due to potassium insertion.

As found for sodium-ion, maximal K^+ inclusion is achieved at the smallest phosphate suspension of 0.75 g/L for pH ranging from 2 to 10. A charge Q around 40 coulombs is carried out in 0.001 and 0.1 M KCl, respectively at a contact time of 2 and 72 h. Therefore, as found for lithium, the diffusion constant in nanoparticles with shortened transport paths is much faster than that in bulk (Yu *et al.*, (2014).

DOI: https://doi.org/10.17509/ijost.v7i2
p- ISSN 2528-1410 e- ISSN 2527-8045

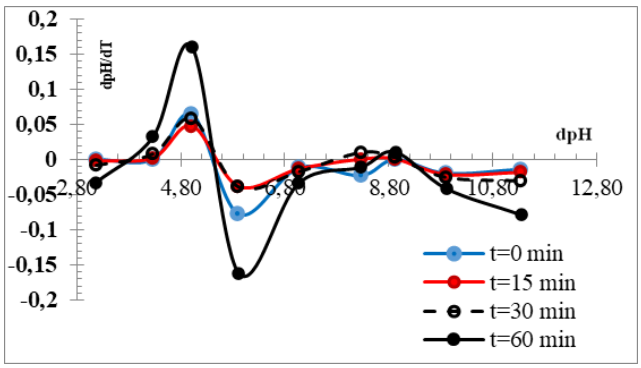

Figure 8. Variation of $\frac{\mathrm{dpH}}{\mathrm{dT}} = \mathrm{f(pH)}$ obtained for m = 0.75 g/L at T ≤ 1h.

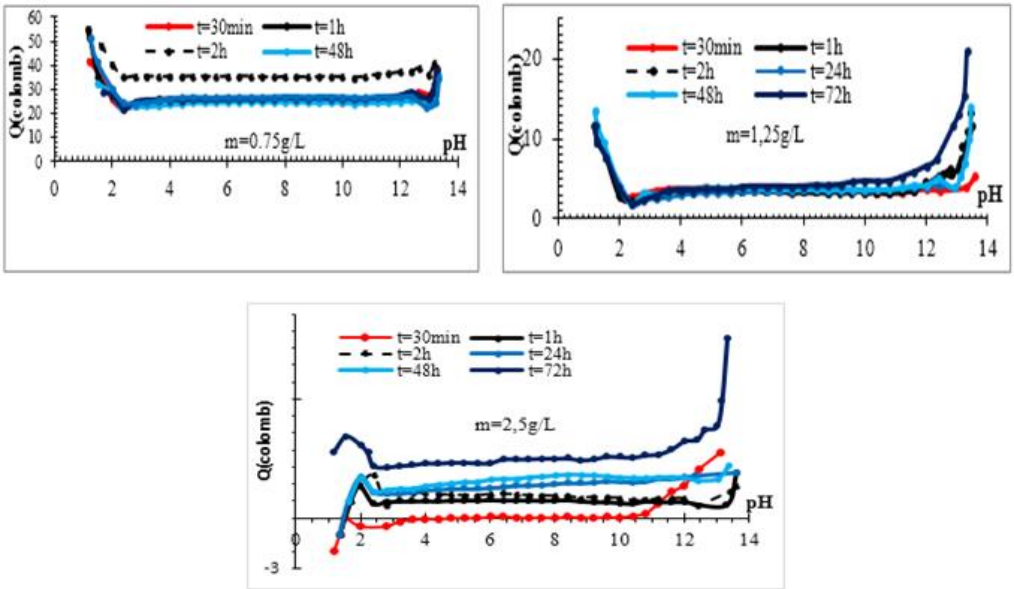

Figure 9. Variation Q = f (pH) for $FePO_4.2H_2O$ in KCl 0.001 M at $0.5h \leq T \leq 72h$ and 0.75 g/L < m < 2.5 g/L.

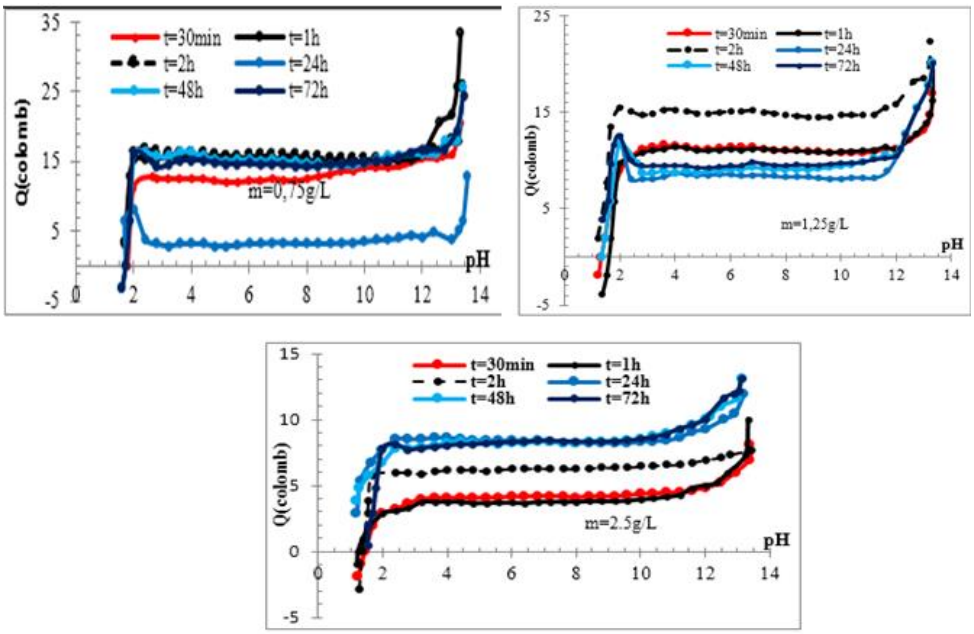

Figure 10: Variation Q = f (pH) for $FePO_4.2H_2O$ in KCl 0.01M at 0.5 h ≤ T ≤ 72 h and 0.75 g/L ≤ T ≤ 2.5 g/L.

DOI: https://doi.org/10.17509/ijost.v7i2
p- ISSN 2528-1410 e- ISSN 2527-8045

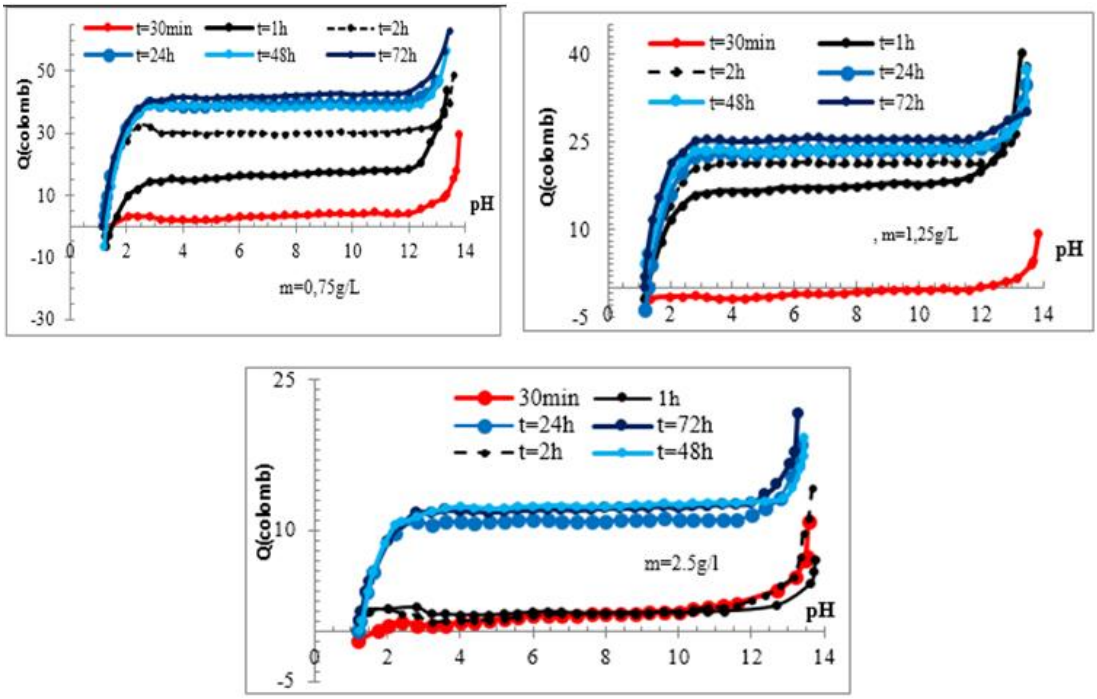

Figure 11. Variation Q = f (pH) for $FePO_4.2H_2O$ in KCl 0.1 M at 0.5 h ≤ T ≤ 72 h and 0.75 g/L ≤ T ≤ 2.5 g/L.

3.5. Surface Complexation Constant

The surface complexation constant for the relationships (1, 2) is, the expression of is simplified and can be written as Equations [4] and [5]:

$$K^{+} = \frac{\left[\overline{> S(\mathrm{OH}_2)^{+}}\right][H^{+}]}{\left[\overline{> \mathrm{SOH}}\right]} \quad (4)$$

$$\mathrm{K}^{-} = \frac{\left[\overline{> \mathrm{SO}^{-}}\right]}{\left[\overline{> \mathrm{SOH}}\right][H^{+}]} \quad (5)$$

pH_{asy} is the asymptotic value of Q=f(pH) variations. Since Q ≥ 0, obtained results allow to obtain $\log(K^{+})$ = - 13.4 ± 0.3.

Taking into account that the suspension activity of "i" specie is $[\bar{\imath}] = 1$, the expression of $K^{\mp}$ is simplified and can be written as Equations [6] and [7]:

$$K^{+} = [H^{+}] \leftrightarrow log(K^{+}) = -\mathrm{pH}_{\mathrm{asy}} \quad (6)$$

$$K^{-} = [H^{+}]^{-1} \leftrightarrow log(K^{-}) = \mathrm{pH}_{\mathrm{asyp}} \quad (7)$$

pH_{asy} is the asymptotic value of Q = f(pH) variations. Since $Q \geq 0$, obtained results allow to $\log(K^{+})$ = -13.4 ± 0.3.

3.6. Computational Methods

The $FePO_4$ lattice was obtained from the Materials Project database as a triclinic crystal system with the P1 symmetry, a density of 3.19 g/cm^3, and a band-gap of 2.491 eV. The Na^+ and K^+ ions were generated with the MarvinSketch software, which supports the widest selection of industrially acknowledged standard chemical file formats. Finally, the loading of ions in the $FePO_4$ lattice was predicted with the Sorption module in the Materials Studio 6.0 software (Akkermans *et al.*, (2013). In particular, the Metropolis Monte Carlo method was implemented with a lower fugacity of 1 atm (101.325 kPa) and an upper fugacity of 10 atm (1013.25 kPa). The temperature was set to 298 K. The sorption was simulated using the COMPASS force field with electrostatic and van der Waals summation methods. Finally, the temperature was set to 298 K; and the sample and grid intervals were set to 50 and 0.4 Å, respectively.

DOI: https://doi.org/10.17509/ijost.v7i2
p- ISSN 2528-1410 e- ISSN 2527-8045

3.6.1. Results

To generate a more realistic curve for the adsorption isotherms, the finer-grained settings were used in the experiment. In a typical case, the curve will rise toward a saturation point value beyond, in which no more molecules can be adsorbed. The adsorption isotherm of Na^+ and K^+ ions in the $FePO_4$ triclinic lattice displays the adsorption in molecules per cell at each fugacity (**Figure 12** [A]), which is better for sodium ions.

This will cause the adsorption energy of Na^+ ions to be significantly more negative compared to the adsorption energy of less strongly bonded potassium ions (**Figure 12** [B]). Additionally, a surface of constant density for Na^+ and K^+ ions was visualized to reveal their favorable binding sites in the lattice framework, where more binding sites were also detected for the sodium ion (**Figure 13** [A, B]).

4. CONCLUSION

A low crystallized iron phosphate ($FePO_4.2H_2O$) powder was synthesized using an inorganic sol-gel method assisted with the microwave route. The zero charges (PZC) and isoelectric point (IEP) of synthesized phosphate were determined by the derivative potentiometric titration technique. The point of zero charge/isoelectric point value was determined to be 4.7. The surface charge time titration method was performed to study the insertion of sodium and potassium ions in the synthesized $FePO_4.2H_2O$. For this purpose, the ionic strength μ was varied between 0.001 and 0.1. Obtained results show that Na^+ and K^+ are time and mass suspension dependent. A maximal insertion of 40 coulombs was achieved at m = 0.75 g/L and μ= 0.001 and 01.

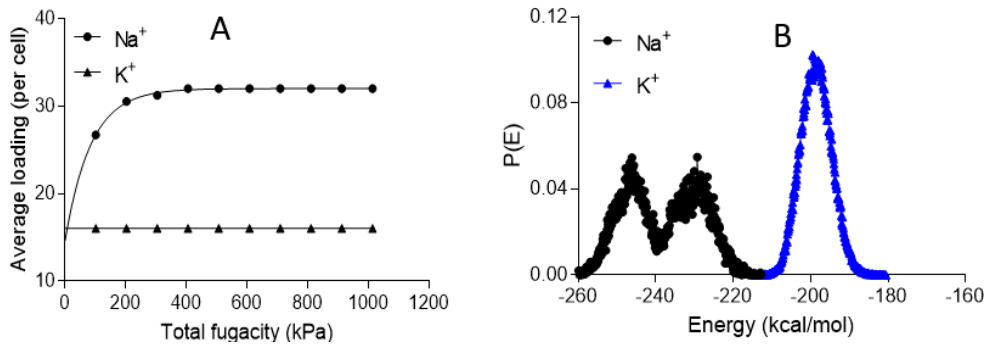

Figure 12. Adsorption isotherms (A) and energy distribution profiles (B) for Na^+ and K^+ ions in the $FePO_4$ triclinic lattice. Linear and non-linear curve fitting methods were utilized to produce the isotherm curves.

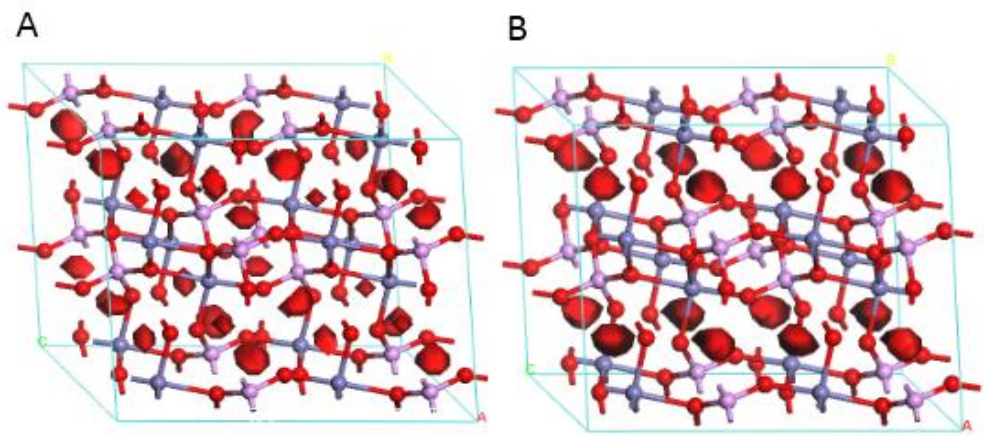

Figure 13: Isodensity surface colored by the potential energy for Na^+ (A) and K^+ (B) ions in the $FePO_4$ triclinic lattice.

DOI: https://doi.org/10.17509/ijost.v7i2
p- ISSN 2528-1410 e- ISSN 2527-8045

5. AUTHORS' NOTE

The authors declare that there is no conflict of interest regarding the publication of this article. The authors confirmed that the paper was free of plagiarism.

6. REFERENCES

Abram, U., and Alberto, R. (2006). Technetium and rhenium: coordination chemistry and nuclear medical applications. *Journal of the Brazilian Chemical Society*, *17*, 1486-1500.

Ai, M., and Ohdan, K. (1999). Effects of the method of preparing iron orthophosphate catalyst on the structure and the catalytic activity. *Applied Catalysis A: General*, *180*(1-2), 47-52.

Akkermans, R. L., Spenley, N. A., and Robertson, S. H. (2013). Monte Carlo methods in materials studio. *Molecular Simulation*, *39*(14-15), 1153-1164.

Berzina-Cimdina, L., and Borodajenko, N. (2012). Research of calcium phosphates using Fourier transform infrared spectroscopy. *Infrared Spectroscopy-Materials Science, Engineering and Technology*, *12*(7), 251-263.

Cappuyns, V., and Swennen, R. (2008). The use of leaching tests to study the potential mobilization of heavy metals from soils and sediments: a comparison. *Water, Air, and Soil Pollution*, *191*(1), 95-111.

De Tommaso, G., and Iuliano, M. (2012). Acid–Base Properties of the Surface of Hydrous Ferric Phosphate in Aqueous Solutions. *Journal of Chemical and Engineering Data*, *57*(1), 52-59.

Destainville, A., Champion, E., Bernache-Assollant, D., and Laborde, E. (2003). Synthesis, characterization and thermal behavior of apatitic tricalcium phosphate. *Materials Chemistry and Physics*, *80*(1), 269-277.

Ellouzi, K., Elyahyaoui, A., and Bouhlassa, S. (2016). Calcium and strontium hydroxyapatites: Microwave accelerated inorganic sol-gel synthesis, and potentiometric determining of the Point of Zero Charge (PZC) and isoelectric point (IEP). *The Pharma Letter*, *8*, 237-245.

Elyahyaoui, A., Ellouzi, K., Al Zabadi, H., Razzouki, B., Bouhlassa, S., Azzaoui, K Mejdoubi, E.M., Hamed, O., Jodeh, S. and Lamhamdi, A., (2017). Adsorption of chromium (VI) on calcium phosphate: mechanisms and stability constants of surface complexes. *Applied Sciences*, *7*(3), 222.

Errich, A., Azzaoui, K., Mejdoubi, E., Hammouti, B., Abidi, N., Akartasse, N., Benidire, L., Hajjaji, S.E., Sabbahi, R. and Lamhamdi, A. (2021). Toxic heavy metals removal using a hydroxyapatite and hydroxyethyl cellulose modified with a new Gum Arabic. *Indonesian Journal of Science and Technology*, *6*(1), 41-64.

Gabaudan, V., Monconduit, L., Stievano, L., and Berthelot, R. (2019). Snapshot on negative electrode materials for potassium-ion batteries. *Frontiers in Energy Research*, *7*, 46.

DOI: https://doi.org/10.17509/ijost.v7i2
p- ISSN 2528-1410 e- ISSN 2527-8045

Gongyan, W., Li, L., and Fang, H. (2018). Dehydration of FePO 4· 2H 2 O for the synthesis of LiFePO 4/C: effect of dehydration temperature. *International Journal of Electrochemical Science*, *13*, 2498-508.

Han, J. K., Song, H. Y., Saito, F., and Lee, B. T. (2006). Synthesis of high purity nano-sized hydroxyapatite powder by microwave-hydrothermal method. *Materials Chemistry and Physics*, *99*(2-3), 235-239.

Ikram, U., Khalida, A., Kausar, I., and Arshia, S.F. (1998). Effect of phosphate enrichement on the metal adsorption Properties of hydrous iron oxide. *Journal of the Chemical Society of Pakistan, 20*(2), 99-109.

Jarlbring, M., Gunneriusson, L., and Forsling, W. (2005). Protolytic Surface Reactions of a Fluorapatite− Maghemite Mixture in Aqueous Suspension. *Langmuir*, *21*(17), 7717-7721.

Jarlbring, Sandstrtim, D.E., Antzutkin, O.N., Holmgren, A., and Forsling, W. (2006). The surface properties of aqueous fluorapatite and maghemite with reference to the dephosphorization of magnetite. *Proceedings of the International Seminar on Mineral Processing Technology, Chennai, India, 270 - 277.*

Kandori, K., Kuwae, T., and Ishikawa, T. (2006). Control on size and adsorptive properties of spherical ferric phosphate particles. *Journal of Colloid and Interface Science*, *300*(1), 225-231.

Kang, B., and Ceder, G. (2009). Battery materials for ultrafast charging and discharging. *Nature*, *458*(7235), 190-193.

Lee, A. Y. W., Lim, S. F., Chua, S. N., Sanaullah, K., Baini, R., and Abdullah, M. O. (2017). Adsorption equilibrium for heavy metal divalent ions (Cu2+, Zn2+, and Cd2+) into zirconium-based ferromagnetic sorbent. *Advances in Materials Science and Engineering*, *2017*, 1-13.

Lee, J. H., Kim, H. H., Kim, G. S., Zang, D. S., Choi, Y. M., Kim, H., Yi, D.K., Sigmund, W.M. and Paik, U. (2010). Evaluation of surface acid and base properties of LiFePO4 in aqueous medium with pH and its electrochemical properties. *The Journal of Physical Chemistry C*, *114*(10), 4466-4472.

Lenoble, V., Laclautre, C., Deluchat, V., Serpaud, B., and Bollinger, J. C. (2005). Arsenic removal by adsorption on iron (III) phosphate. *Journal of Hazardous Materials*, *123*(1-3), 262-268.

Li, X., Xiao, X., Li, Q., Wei, J., Xue, H., and Pang, H. (2018). Metal (M= Co, Ni) phosphate based materials for high-performance supercapacitors. *Inorganic Chemistry Frontiers*, *5*(1), 11-28.

Lozano-Calero, D., Bruque, S., Aranda, M. A., Martinez-Lara, M., and Moreno, L. (1993). Topotactic Lithium Exchange in the Precursor Catalyst VOHPO4· 0.5 H2O: The Crystal Structure of LiVOPO4· 0.5 H2O. *Journal of Solid State Chemistry*, *103*(2), 481-489.

Maarouf, F. Z., Saoiabi, Z., Azzaoui, K., Chrika, C., Khalil, H., Elkaouni, S., Lhimr, S., Boubker, O., Hammouti, B., and Jodeh, S. (2021). Statistical optimization of amorphous iron phosphate : inorganic Sol-gel synthesis -sodium potential insertion, *MC Chemistry*, *15*, 48-63.

DOI: https://doi.org/10.17509/ijost.v7i2
p- ISSN 2528-1410 e- ISSN 2527-8045

Meejoo, S., Maneeprakorn, W. and Winotai, P, (2006). Phase and thermal stability of nanocrystalline hydroxyapatite prepared via microwave heating. *Thermochimica Acta, 447,* 115-120.

Mobasherpour, I. and Heshajin, M. (2007). Synthesis of nanocrystalline hydroxyapatite using precipitation method. *Journal of Alloys and Compounds, 430,* 330 – 333.

Moradi, M., Li, Z., Qi, J., Xing, W., Xiang, K., Chiang, Y. M., and Belcher, A. M. (2015). Improving the capacity of sodium ion battery using a virus-templated nanostructured composite cathode. *Nano Letters*, *15*(5), 2917-2921.

Muhammad, S. T. H. S., Hussain, S. T., Waseem, M., Naeem, A., Hussain, J., and Tariq Jan, M. (2012). Surface charge properties of zirconium dioxide. *Iranian Journal of Science and Technology (Sciences)*, *36*(4), 481-486.

Mustafa, S., Javid, M., and Zaman, M. I. (2006). Effect of activation on the sorption properties of AlPO4. *Separation Science and Technology*, *41*(15), 3467-3484.

Mustafa, S., Naeem, A., Murtaza, S., Rehana, N., and Samad, H. Y. (1999). Comparative sorption properties of metal (III) phosphates. *Journal of Colloid and Interface Science*, *220*(1), 63-74.

Naeem, S., Mustapha, S., Murtaza, B., DilAra, A., and Hamid, (2001). Temperature effect on ion exchange behavior of aluminum (IV) phosphate. *Journal of the Chemical Society*, *23*(3), 133-136.

NaeemáKhan, A. (1993). Cation-exchange properties of iron (III) phosphate. *Journal of the Chemical Society, Faraday Transactions*, *89*(20), 3843-3848.

Nilsson, L., Lövgren, S., and Sjöberg, (1992). Phosphate complexation at the surface of goethite, *Chemical Speciation and Bioavailability, 4*(4), 121-130**.**

Palacios, E., Leret, P., Fernández, J. F., De Aza, A. H., and Rodríguez, M. A. (2012). Synthesis of amorphous acid iron phosphate nanoparticles. *Journal of Nanoparticle Research*, *14*(10), 1-7.

Pan, H., Hu, Y. S., and Chen, L. (2013). Room-temperature stationary sodium-ion batteries for large-scale electric energy storage. *Energy and Environmental Science*, *6*(8), 2338-2360.

Ramesh, P., Anteneh, M.B., and Do Kyung, K. (2019). Phosphorus-derived compounds for Li and Na ion batteries. *Research and Development in Material Science, 10*(4).

Raynaud. S., Champion. E., Bernache-Assollant. D., and Thomas. P. (2002). Calcium phosphate apatites with variable Ca/P atomic ratio I. Synthesis, characterisation and thermal stability of powders. *Biomaterials*, *23*(4), 1065-1072**.**

Razzouki, B., El Hajjaji, S., Azzaoui, K., Errich, A., Lamhamdi, A., Berrabah, M., and Elansari, L. L. (2015). Physicochemical study of arsenic removal using iron hydroxide. *Journal of Materials and Environmental Science*, *6*(5), 144-1450.

DOI: https://doi.org/10.17509/ijost.v7i2
p- ISSN 2528-1410 e- ISSN 2527-8045

Salamani, A., Merrouche, L., Telli, P., Gómez-Romero, Z. C., and Huertas, (2018). Synthesis and caracterization of mesoporous fepo4 as positive electrode materials for lithium batteries. *Surface Engineering and Applied Electrochemistry, 54*(1), 55–63.

Song, Y., Zavalij, P. Y., Suzuki, M., and Whittingham, M. S. (2002). New iron (III) phosphate phases: crystal structure and electrochemical and magnetic properties. *Inorganic Chemistry*, *41*(22), 5778-5786.

Tejedor-Tejedor, M. I., and Anderson, M. A. (1990). The protonation of phosphate on the surface of goethite as studied by CIR-FTIR and electrophoretic mobility. *Langmuir*, *6*(3), 602-611.

Thinnappan, V., Merrifield, C. M., Islam, F. S., Polya, D. A., Wincott, P., and Wogelius, R. A. (2008). A combined experimental study of vivianite and As (V) reactivity in the pH range 2–11. *Applied Geochemistry*, *23*(11), 3187-3204.

Vinod, l., Jungwon, K., Jihyeon, G., Jinju, S., Joseph, P., Baboo, J., Park, J., Docheon, A., Junhee, H., Lin, G., Yuesheng, W., Yong, S.H., Yang, K.S., and Jaekook, K. (2015). Amorphous iron phosphate: potential host for various charge carrier ions. *Asia Materials*, *7*, 149.

Wang, H., Liu, L., Wang, R., Zhang, D., Zhu, L., Qiu, S., Wei, Y., Jin, X. and Zhang, Z. (2015). Design and synthesis of high performance LiFePO 4/C nanomaterials for lithium ion batteries assisted by a facile H+/Li+ ion exchange reaction. *Journal of Materials Chemistry A*, *3*(15), 8062-8069.

Wang, Y., Persson, P., Michel, F. M., and Brown Jr, G. E. (2016). Comparison of isoelectric points of single-crystal and polycrystalline α-Al2O3 and α-Fe2O3 surfaces. *American Mineralogist*, *101*(10), 2248-2259.

Yu, F., Zhang, L., Li, Y., An, Y., Zhu, M., and Dai, B. (2014). Mechanism studies of LiFePO 4 cathode material: lithiation/delithiation process, electrochemical modification and synthetic reaction. *RSC Advances*, *4*(97), 54576-54602.

Zhang, W., Liu, Y., and Guo, Z. (2019). Approaching high-performance potassium-ion batteries via advanced design strategies and engineering. *Science Advances*, *5*(5), eaav7412.

Zhang, X. X., Tang, S. S., Chen, M. L., and Wang, J. H. (2012). Iron phosphate as a novel sorbent for selective adsorption of chromium (III) and chromium speciation with detection by ETAAS. *Journal of Analytical Atomic Spectrometry*, *27*(3), 466-472.

Zhang, X., Zhang, Z., Yao, S., Chen, A., Zhao, X., and Zhou, Z. (2018). An effective method to screen sodium-based layered materials for sodium ion batteries. *NPJ Computational Materials*, *4*(1), 1-6.

Zhu, X. F., Lan, J., and Kwon, O. (2003). An expedient phosphine-catalyzed [4+ 2] annulation: synthesis of highly functionalized tetrahydropyridines. *Journal of the American Chemical Society*, *125*(16), 4716-4717.

DOI: https://doi.org/10.17509/ijost.v7i2
p- ISSN 2528-1410 e- ISSN 2527-8045